ELSEVIER

Soil & Tillage Research 56 (2000) 131–144

Soil & Tillage Research

www.elsevier.com/locate/still

Raindrop erosion of tillage induced microrelief: possible use of the diffusion equation

Olivier Planchon[a,*], Michel Esteves[b], Norbert Silvera[a], Jean-Marc Lapetite[b]

[a]

[b]

Received 6 July 1999; received in revised form 17 May 2000; accepted 5 June 2000

Abstract

The purpose of this paper is to evaluate the possibility of using the diffusion equation for raindrop erosion modelling. We wanted in particular to know if such a model could provide accurate interpolations of microrelief between two known dates. In a theoretical section, we show that the assumption that soil particles follow parabolic trajectories when splashed by raindrop impacts leads to a diffusion equation. This equation suggests a linear relation between Δ , the variation of height between two dates, and the Laplacian ∇^2 ($\nabla^2 = \partial^2/\partial^2 + \partial^2/\partial^2$). This relation is confirmed by data from a simulated rainfall experiment carried out in the sandy soils of the Senegalese groundnut belt. Four square plots of side 4 m each were used. They were hoed with a traditional horse-drawn three-tined hoe. Three rains of 70 mm h^{-1} lasting 30 min each were applied. An automated relief meter designed and constructed by the authors was used to measure the distribution of heights for every 5 cm before the first rain, and after the first and the third rains. The mean correlation coefficient of the model was 62% for the first rain and 46% for the next two rains. Besides raindrop erosion, compaction occurred during the first rain. Adding a crude description of compaction enhanced the mean of the correlation coefficients of the model up to 70% for the first rain. Furthermore, the coefficient of variation of the four adjusted total diffusion lessens from 10 to 6%. The simulated surfaces were smoother than the real ones, which was an expected result, but the surface storage capacity was overestimated. The latter result illustrates the role of runoff in shaping the flow paths it follows and, consequently, in lessening the surface storage capacity. The main conclusion is that the diffusion equation provides a promising frame for further development of models simulating microrelief evolution during rainfall. Another conclusion is that these models should integrate existing routines for runoff erosion at small scale in order to simulate surfaces with realistic hydraulic properties. © 2000 Published by Elsevier Science B.V.

Rainfall simulation; Microrelief; Raindrop erosion; Senegal

1. Introduction

The lack of accuracy of erosion models currently used is now recognised. (Bjorneberg et al., 1997; Boardman and Favis-Mortlock, 1998; Nearing, 1998; Jetten et al., 1999). Jetten et al. (1999) have tested seven models at the scale of the small watershed and the rainstorm. Despite a reasonable confidence in the predicted peak hydrographs and in the total runoff, soil loss predictions were dramatically poor. Among other conclusions, the authors recommended integration of the interactions between microrelief, runoff and erosion in the models.

Practically all the surface properties of cultivated soils, and their evolution with the cumulated rainfall, have been intensively studied so that an extensive

* Corresponding author. Present address: IRD, BP 1386, Dakar, Senegal. Tel.: +221-849-35-35; fax: +221-832-43-07.
: olivier.planchon@ird.sn (O. Planchon).

0167-1987/00/$ – see front matter © 2000 Published by Elsevier Science B.V.
PII: S0167-1987(00)00134-3

Nomenclature

	distance of impact of a particle with a virtual horizontal plane
	flux of soil along the slope
( )	parabolic trajectory equation of a splashed particle
	total diffusion during Δ
	mean coefficient of diffusion for all the splashed particles and all the trajectories
(θ)	variation of horizontal co-ordinate of the centre of gravity of two equal masses splashed in opposite directions on a surface with a slope θ (negative if the slope is positive)
	mass of soil detached per unit time and surface area
(θ)	horizontal distance of the splash projection on a surface with a slope θ
Δ	duration of the rainfall between two measurements
	volume of soil detached per unit time and surface area
	mean height of the plot
Δ	mean variation of the height of the plot between two measurements
	height of a given point in the plot
Δ	variation of height of a given point during Δ
∇^2	Laplacian of : $\partial^2/\partial^2+\partial^2/\partial^2$
RR	random roughness (mm)
SSA	specific surface area (%)
SSC	surface storage capacity (mm)
α	splash angle $0\leq\alpha<\pi/2$ (0=horizontal)
γ	rate of compaction (final over initial bulk density)
λ	depth of tillage
θ	slope angle, $\mathrm{tg}(\theta)=\partial/\partial$
ρ	bulk density of the detached soil

review of these works would be lengthy. The covered topics begin with the early stages of aggregate slaking (Boiffin, 1984; Le Bissonnais et al., 1998) and their consequences on surface roughness (Helming et al., 1998). The next stages of soil sealing and crusting have been classified (Valentin and Bresson, 1992, 1997). Most of the geometric properties of soil surface have been monitored through successive rainstorms (Roth and Helming, 1992; Magunda et al., 1997; Kamphorst et al., 2000). All these works highlight the fast evolution of soil surface properties. Magunda et al. (1997) reported, e.g., an exponential decay of random roughness with cumulated rainfall. This changeability is a great obstacle to the application of the recommendations of Jetten et al. (1999) to integrate them in the soil erosion models. Therefore, we can see the importance of a model able to interpolate the microrelief between an initial and a final stage. This paper presents the first step towards such a model.

In a theoretical section, we first establish that the diffusion equation can represent the effect of splash caused by raindrop impacts on microtopography. The objective of this preliminary study was to evaluate the pertinence of the diffusion equation. For that purpose, we have analysed three simulated rainfalls performed on four plots. A simplified form of the diffusion equation was calibrated from the variations of surface elevation (initial surface before the rainfall and final surface after the rainfall). The final surfaces were then calculated with the calibrated coefficients and the adequacy of the calculated surface to the measured one was evaluated according to: (a) the criterion for the percent of the variance of the variation of heights explained and (b) some geometric properties of the simulated surfaces such as random roughness (RR), specific surface area (SSA) and surface storage capacity (SSC). Possible developments towards a model that fully simulates the evolution of soil microtopography under rainfall are then discussed.

2. Material and methods

The experiment took place in a 2.85 ha catchment of Thysse Kaymor, a village of the Senegalese groundnut belt. The median slope gradient is 0.73% and 95% of the catchment has a slope gradient below 1.5%. The area is cultivated with millet–groundnut rotation. Tillage is horse-drawn, perpendicular to the slope, and spaced at every 50 cm in groundnut and at every meter in millet (Perez, 1994).

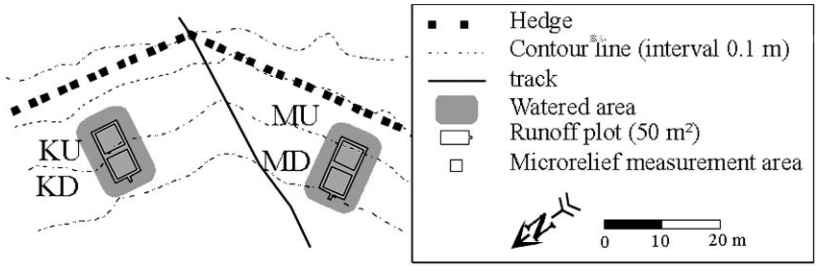

Fig. 1. Situation map.

For this experiment, we used four plots of 4 m×4 m, grouped by pairs into two larger rainfall simulation plots of 5 m×10 m. The rainfall simulation plots were called K and M. Two letters were used to call each single plot: K or M, for the main plot, followed by U or D, for the position in the main plot: up or down. The D plots received runoff from the U plots. This design was required for another experiment, carried out simultaneously and dealing with the spread of nematodes by runoff (Planchon et al., 2000a), but could have unwanted effects when studying raindrop erosion. As explained below, KU plot was the replicate of MD plot and conversely, KD was the replicate of MU, so that the verification of a possible bias caused by runoff from upstream could be done. Plots K and M are 30 m from each other and have the same sandy soil, with 60% of sand and 6% of clay. Fig. 1 shows the overall arrangement of the experiment.

The experiment was carried out in April, 2 months before the beginning of the rainy season. The soil surface was initially dry, bare and smooth. During the 2 weeks preceding the first rain of the experiment, three rains of 10 mm each were applied on each plot. This allowed us to reproduce the moisture conditions which are the most common to that area before hoeing. The day before the first rain, plots MU and KD were hoed at a 50 cm interval with a traditional hoe called 'Houe Sine'. This tool commonly works at a depth between 5 and 10 cm (Perez, 1994). Microrelief was measured after hoeing. Rains 1 and 2 were applied in these conditions. Then, the unworked plots were hoed the same way. The soil was more humid than when the first plots were tilled and was easier to work. The soil surface after hoeing was therefore slightly rougher for these two plots. A third and last rain was applied in these conditions. Each rain was about 35 mm depth. Table 1 gives the time schedule and the rainfall characteristics.

In summary, MU and KD are two replicates of three consecutive rainfalls on a sandy soil hoed in the most

Table 1
Time schedule and rainfall characteristics

Day	Rainfall (mm) [mm h^{-1}]				KD and MU	KU and MD
	KD	MU	KU	MD		
1	10	10	10	10		
6	10	10	10	10		
11	10	10	10	10		
16						Microrelief measurement
17					Hoeing, microrelief measurement	
18	38, [76]	29, [58]	41	32	Rain 1	
19					Microrelief measurement	
20	38, [76]	33, [66]	41	32	Rain 2	35 mm rain
21						Hoeing, microrelief measurement
22	37, [73]	37, [74]	40, [80]	34, [69]	Rain 3	Rain 1
23					Microrelief measurement	
24						Microrelief measurement

common conditions to that area (30 mm antecedent rainfall) and MD and KU are two replicates of a single rainfall on the same soil, hoed in a more humid condition (90 mm antecedent rainfall), which generated slightly rougher soil surfaces.

A new rainfall simulator has been designed for this experiment by the authors (Esteves et al., 2000). The basic unit of the simulator is a vertical galvanised standpipe of 6.6 m in height and 1 in. in diameter. A HQ106 spraying system nozzle is screwed onto the top of the pipe, spraying upwards. Lacano et al. (1997) evaluated the raindrop characteristics of the nozzle used when developing their own rainfall simulator. At a water pressure of 41.18 kPa the mean drop diameter was 2.4 mm and the calculated kinetic energy was 23.5 J m^{-2} mm^{-1}. A valve and an oil-immersed pressure gauge allows fine control of pressure at the bottom of each pipe. Each basic unit waters a square area of 8 m×8 m. A distance of 5.5 m between two single units gives the best uniformity of rainfall and a mean rainfall intensity of 35 mm h^{-1}. Two lines of three units each were used to simulate rainfall in each plot. The amount and uniformity of simulated rainfalls were measured using collecting cans, placed at each square metre inside the plots.

The relief meter (Fig. 2) was designed and constructed by the authors at the IRD research centre in Dakar, Senegal (Planchon et al., 2000b). This device is fully automatic. It is made of a carriage which moves on a transversal beam and which supports and controls a vertical rod, with a sensor at the end. The rod moves vertically downwards until the sensor contacts the soil surface. The beam moved on a transportable frame, 4.5 m wide and 1.2 m high, screwed to four bases anchored at a depth of 50 cm in the ground. The stability of the bases was verified by measurements of the height of each frame corner after each rainfall. The anchored bases allowed measurement of almost the same points from rain to rain. During the experiment, a certain number of rows were measured twice to determine the accuracy of the measurement. The standard deviation of the heights measurements was 0.85 mm. The standard deviation of the position of the measured points was 3 mm.

Random roughness (RR) was defined as the standard deviation of heights after the slope and tillage effects were removed and the upper and lower 10% of the measurements were eliminated (Allmaras et al., 1966). They used a logarithm transformation of the raw data but the pertinence of this transformation was contested later (Currence and Lovely, 1970). Moreover, Zobeck and Onstad (1987) pointed out that it is sometimes difficult to determine whether or not all details of the Allmaras et al. (1966) procedure were carried out in a given study. In our study, the slope and tillage effects were corrected with both the means of current row and current column. RR is the standard deviation of the corrected heights. The following equation provides the formula used:

$$\mathrm{RR} = \sqrt{\frac{\sum_{,} (\ ,\ -\ _{,\cdot} -\ _{\cdot,} +\ _{\cdot,\cdot})^2}{\ -1}} \tag{1}$$

where and are rows and columns indexes; $_{,\cdot}$, $_{\cdot,}$, $_{\cdot,\cdot}$ are the mean value of row , column , and all the data, respectively, and is the number of cells.

Specific surface area (SSA) was calculated as the microrelief surface area over the horizontal projected area minus one (Helming et al., 1998). For this calculation, each 5 cm×5 cm cell was supposed to have a bilinear surface of Eq. (2). The area follows Eq. (3) which has been integrated and translated into C code by Mapple V™. SSA is in percent.

$$(\ ,\ ) = \quad + \quad + \quad + \tag{2}$$

$$= \int_0^{\Delta} (1 + \ ^2 + 2 \quad + \ ^2\ ^2)^{1/2}\,\mathrm{d}$$

$$\times \int_0^{\Delta} (1 + \ ^2 + 2 \quad + \ ^2\ ^2)^{1/2}\,\mathrm{d} \tag{3}$$

where Δ and Δ are the cell sizes along rows and columns of the DEM, respectively.

The method used to calculate surface storage capacity (SSC) was described by Planchon and Darboux

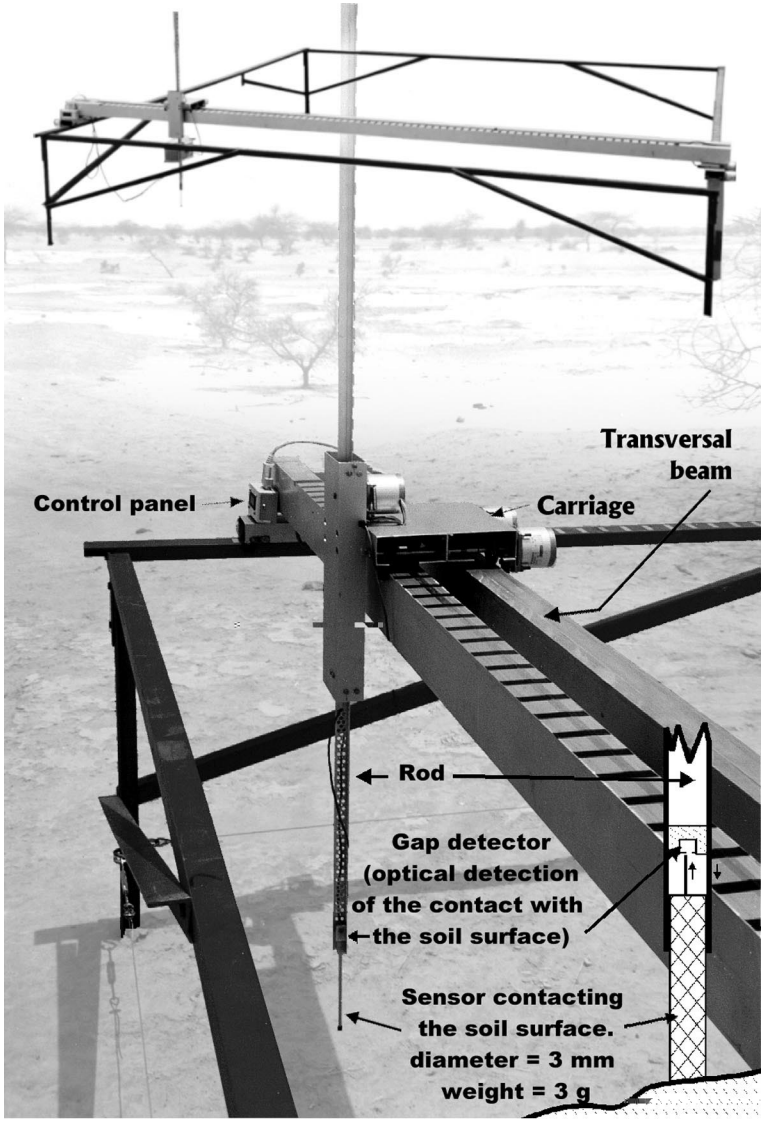

Fig. 2. The relief meter.

(2000). Each cell represents a small square horizontal area and the method considers eight neighbours for each cell. These two points have been widely adopted after the work of Moore and Larson (1979). Contrary to the other methods (Moore and Larson, 1979; Jenson and Domingue, 1988) which gradually fill depressions and merge the embedded ones, this method first adds a thick layer of water on the whole area and then iteratively removes the water in excess. The method gives the same result as Jenson and Domingue (1988) but it is simpler and drastically faster when used in large DEMs with a strong random component.

As the ridges were perpendicular to the slope, SSC was sensitive to boundary condition. We used a three-wall boundary condition (up, left and right), which is the most commonly used in that case (Kamphorst et al., 2000). SSC is in millimetres. As ridges are perpendicular to the slope direction, this boundary condition emphasises the variations in SSC caused by runoff eroding the ridges when crossing them.

3. Raindrop erosion model

The trajectory of a splashed particule can be assimilated to a parabola of

$$( ) = \left(1 - -\right)\mathrm{tg}(\alpha) \tag{4}$$

where α is the angle of projection and is the distance of projection on an horizontal plane (Fig. 3).

On a sloping area with a slope angle θ, the distance of projection (θ), is the root of Eq. (5) which is the equation of the intersection between the parabola $= ( )$ and the straight line $=\ \mathrm{tg}(\theta)$:

$$(\ (\theta)) = \ (\theta)\,\mathrm{tg}(\theta) \tag{5}$$

i.e.

$$(\theta)\,\mathrm{tg}(\theta)\left(1 - \frac{(\theta)}{}\right) = \ (\theta)\,\mathrm{tg}(\theta) \tag{6}$$

from which we deduce

$$(\theta) = \ \left(1 - \frac{\mathrm{tg}(\theta)}{\mathrm{tg}(\alpha)}\right) \tag{7}$$

If two equal masses are simultaneously projected up and down, (θ), given by Eq. (8), is the horizontal displacement of the centre of gravity of the two masses;

$$(\theta) = \ (\theta) - \ (-\theta) \tag{8}$$

which leads to

$$(\theta) = -2\ \frac{\mathrm{tg}(\theta)}{\mathrm{tg}(\alpha)} \tag{9}$$

Negating the time between detachment and deposit of a particle, and denoting $_{\alpha,}$ as the total mass of two lumps of soil of equal masses which are projected in opposite directions with trajectories characterised by $(-\alpha, \ )$ and $(\alpha, \ )$, the centre of gravity of $_{\alpha,}$ covers a length (θ) per unit time. The mass flux $_{\alpha,}$ of these two lumps of soil is therefore the product $_{\alpha,}$ by (θ). Expanding (θ) and substituting $\mathrm{tg}(\theta)$ by $\partial\ /\partial$, leads to the following equation:

$$_{\alpha,} = \frac{-\ _{\alpha,}}{\mathrm{tg}(\alpha)}\frac{\partial}{\partial} \tag{10}$$

where $_{\alpha,}$ is the mass detached per unit time and surface area (kg m^{-2} s^{-1}) following a trajectory $(\alpha, \ )$.

During rainfall the distance of projection depends upon the particle size (Savat and Posen, 1981) and the projection angle α depends upon the water depth on the soil surface, among other parameters (Al Durrah and Bradford, 1982). The resulting flux is the sum, over all the possible trajectories, of their respective fluxes. Integrating Eq. (10) for all possible trajectories leads to

$$= -\ \ \frac{\partial}{\partial} \tag{11}$$

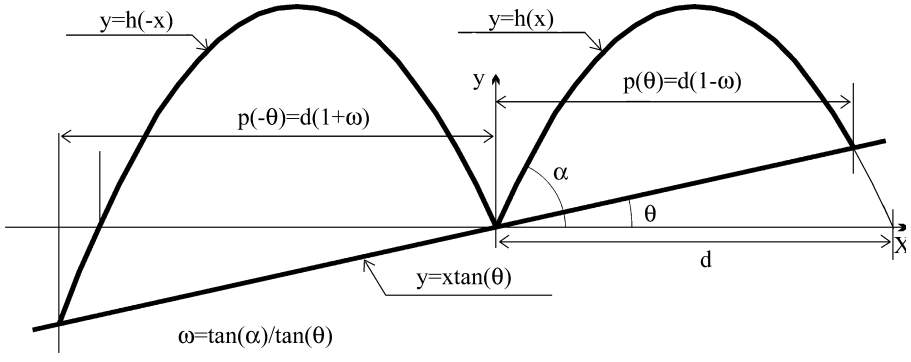

Fig. 3. Diagram of the parabolic trajectories of the splashed particules. Notations are those of Eqs. (4)–(7).

where

$$= \int_{=0}^{\infty} \int_{\alpha=0}^{\pi/2} \left(\frac{_{\alpha,}}{\mathrm{tg}(\alpha)} \right) \mathrm{d}\alpha \, \mathrm{d}$$

In this integral, $_{\alpha,} = 0$ if α is less than the slope. This highlights the fact that, as discussed in the above paragraph, $_{\alpha,}$ is not uniform, neither in time, nor in space. As a result, this property is passed on .

Mass conservation leads to Eq. (12), the continuity equation

$$\frac{\partial(\rho\ )}{\partial} = -\frac{\partial}{\partial} \tag{12}$$

where ρ is the bulk density of the soil and the height of the soil surface.

Combining Eqs. (11) and (12) leads to the following equation:

$$\frac{\partial(\rho\ )}{\partial} = \frac{\partial}{\partial} \left(\quad \frac{\partial}{\partial} \right) \tag{13}$$

whose expanded form is

$$\rho \frac{\partial}{\partial} + \frac{\partial \rho}{\partial} = \quad \frac{\partial^2}{\partial\ ^2} + \frac{\partial(\quad)}{\partial} \frac{\partial}{\partial} \tag{14}$$

Up to this point, we have made no simplifications, and Eq. (14) is a rigorous description of the complex phenomenon taking place when lumps of soil are projected into the air under the impact of rain drops. The only restriction is that we are concerned only with soil transport due to splashes and do not take into account other possible means of transport such as overland flow in this study.

In order to reduce Eq. (14) into a simpler partial differential equation, we need to make two assumptions. The validity of these assumptions is presently impossible to demonstrate using a physical reasoning. It is one of the purposes of this paper to justify these assumptions by validating the simplified expressions that result from these simplifications.

The first assumption concerns $\partial\rho/\partial$, the compaction term, in order to simplify the left member of Eq. (14). Since we can estimate the compaction between two rains, but not its dynamics during rainfall, we must choose between two simplifying hypotheses. The first would suppose that the compaction rate $\partial\rho/\partial$ is constant; the second would assume that compaction takes place mainly during the very beginning of the rainfall and that raindrop erosion occurs on a compacted soil with $\partial\rho/\partial = 0$. The latter hypothesis is the most suitable for our case because the soils of the experimental area are sandy with low clay and organic matter contents and a low structural stability. Clods generated by tillage therefore disintegrate quickly when the rain begins. A last argument for the latter hypothesis is that the mean elevation of the plots, and therefore the soil's bulk density, changed only during the first rain after tillage and remained constant thereafter, which is in agreement with van Wesemael et al. (1995), who observed that the subsidence of the soil surface stopped after 17.5 mm of rainfall. It is then reasonable to assume that $\partial\rho/\partial = 0$ most of the time. Once this simplification is accepted, we need a method to calculate the hypothetical surface after compaction and before raindrop erosion. Such a method is shown in a later section.

The second assumption concerns the spatial variability of and (Eq. (11)), in order to simplify the right-hand side term of Eq. (14). Although probably not spatially constant, we make it part of our hypothesis that $(\partial\ /\partial\ )(\partial(\quad)/\partial\ )$ is going to be negligible compared to $(\partial^2\ /\partial\ ^2)$. In order to discuss this hypothesis one can consider that the soil surface made of a succession of ridges at every 0.5 m, can be approximated by $\sin(4\pi\ )$ where is the peak amplitude and the co-ordinate, in metres, in the direction across the furrows. From this approximation, the order of magnitude of $\partial\ /\partial$ (respectively, $\partial^2\ /\partial\ ^2$) would be 4π (respectively, 16π). Our initial hypothesis is now equivalent to assuming that $\partial(\quad)/\partial$ is negligible compared to 4π . This is not very restrictive because it just assumes that the spatial variations of are gradual. For instance, coming back to the 0.5 m spaced ridges, a change of the value of of $\pm 10\%$ over 10 cm would not contradict our hypothesis. On a freshly hoed soil, the physical properties of the soil surface are homogeneous and as such would be well within the limits of our constraint. However, the quantity of soil detached by a given raindrop impact is strongly dependent on the depth of the water film at the soil surface. There is therefore the risk that our simplifying hypothesis would not hold up near the edge of a puddle because of the changeable depth of these areas. This being said, these transition areas are not so numerous to the point where they would jeopardise our hypothesis and it is one of the results

of this work to show that despite a few necessary hypothesis, Eq. (14) remains an interesting way to forward model raindrop erosion. The two assumptions discussed above lead to the following simple equation:

$$\frac{\partial}{\partial} = \frac{}{\rho}\nabla^2 \tag{15}$$

where $\nabla^2 = (\partial^2/\partial^2) + (\partial^2/\partial^2)$, Laplacian of , and (/$\rho$) can be assimilated to a diffusion coefficient.

This equation is valid after the compaction has taken place in the very beginning of the rainfall. Note that to establish this equation, we did not have to assume that the bulk density is spatially independent.

The following sections show how to calculate the hypothetical soil surface after compaction and before raindrop erosion. The compaction rate γ was unknown as both the bulk density of the freshly tilled soil and the depth of hoeing were unknown. We therefore made another set of simplifying hypothesis in order to determine the range of the compaction rate γ.

Two depths were simulated: 5 and 10 cm. The real depth of soil work was certainly in this interval (Perez, 1994).

Microrelief was measured before hoeing for MD and KU plots, but not for MU and KD plots (see the time schedule in Table 1). Plots MD and KU were used to validate a method for estimating the initial soil surface, when unknown. The method consists of smoothing the final surface, measured after the last rain, with a moving average on a window of 45 cm each side which is close to the mean interval of the furrows. This method completely removed the shape of the furrows and the initial distribution of height was reproduced with a standard deviation of 5 mm.

γ as given by Eq. (16) expresses the compaction of a layer of depth ($\Delta + \lambda$), which is the depth of the hoed layer before rainfall, into a layer of depth, λ which is the depth of hoeing. Δ is known from data and γ is supposed to be either 5 or 10 cm.

$$\gamma = \frac{\Delta + \lambda}{\lambda} \tag{16}$$

For the four plots and the two scenarios above (hoed at 5 and 10 cm depth, respectively), the distribution of heights after compaction was calculated with Eq. (17):

$$_c = (_0 - \lambda) + \frac{- _0 + \lambda}{\gamma} \tag{17}$$

where $_c$ is the height of a given point after compaction, $_0$ the known (MD and KU), or estimated (MU and KD), height of the point on the initial surface, the known height of the point after soil tillage, λ the estimated depth of hoeing (5 or 10 cm) and γ the compaction coefficient given by Eq. (16).

To the best knowledge of the authors, the diffusion equation has never been applied to the modelling of raindrop erosion. De Ploey and Savat (1968) have already used an equation similar to Eq. (9), but they worked at the slope scale and did not derive a diffusion equation. Because of that the numerical schemes developed for this partial derivative equation are not necessarily the most appropriate. This section explains how ∂/∂ and ∇^2 have been differentiated.

A crude time differentiation of Eq. (15) on the whole duration between two microrelief measurements leads to Eq. (18):

$$\frac{\Delta}{\Delta} = \quad \nabla^2 \tag{18}$$

where Δ is the variation of altitude during the whole rainfall and Δ is the duration of the rainfall.

Eq. (19) is a slightly modified form of Eq. (18) which suggests a linear relation between ∇^2 and Δ :

$$\Delta \; = \quad \nabla^2 \tag{19}$$

where =(/ρ)Δ .

If the relation is found to be actually linear, this would be a strong argument in favour of the use of the diffusion equation to describe the effect of raindrop erosion on tilled sandy soils. The calibration of coefficient would allow us to simulate the effect of raindrop erosion alone on the initial surfaces and to compare the simulated surfaces to the measured ones. A careful comparison of the simulated and measured surfaces would then allow us to evaluate more

precisely the role of raindrop erosion in the evolution of microrelief patterns caused by rainfall.

Eq. (20) shows the classical second-order scheme for ∇^2 when evaluated on a square grid:

$$\nabla^2 = \frac{+1, + -1, + ,+1 + ,-1 - 4 ,}{2} + \mathrm{O}(^2) \tag{20}$$

where , is the height at row and column and is the cell size.

Eq. (21) shows a less classical scheme when the differentiation follows the diagonals instead of the usual rows and columns:

$$\nabla^2 = \frac{+1,+1 + -1,+1 + +1,-1 + -1,-1 - 4 ,}{2\ ^2} + \mathrm{O}(^2) \tag{21}$$

Any linear combination of Eqs. (20) and (21) gives a new second-order scheme. Among them the mean is given by Eq. (22):

$$\nabla^2 = \left(\frac{(+1, + -1, + ,+1 + ,-1)/2 + (+1,+1 + -1,+1 + +1,-1 + -1,-1)/4}{2} - 3 , \right) + \mathrm{O}(^2) \tag{22}$$

This scheme (Eq. (22)) is not often used to differentiate ∇^2 because although it is more complicated than the scheme of Eq. (20), it is still second order in space. Nevertheless, in our application which did not involve calculations for multiple time steps as in a conventional PDE integration, the use of the diagonal neighbours allowed by Eq. (22) led to a significant enhancement of the coefficients of correlation shown in the following section.

Let us call $_0$ and $_1$ the distribution of heights before and after rainfall, respectively, and $_c$ the hypothetical soil surface after compaction and before raindrop erosion. The method described above was first applied ignoring compaction, then repeated for λ=5 and 10 cm. It is summarised in the following five steps:

step 1: calculate Δ from data
step 2: if compaction is not ignored, calculate λ from Eq. (16), then calculate $_c$ according to Eq. (17), elsewhere take $_c = _0 + \Delta$
step 3: calculate ∇^2 on $_c$, according to Eq. (22).
step 4: calculate (Eq. (19)) as the slope of the regression line of ($_1 -$ $_c$) against ∇^2
step 5: calculate the residuals ε and the simulated surface

The correlation coefficient ^{2} of the model can be calculated according to Eq. (23) which shows the percentage of the variance explained by the model.

$$^2 = \frac{\sum(\Delta)^2 - (1/)\sum^2 \Delta - \sum \varepsilon^2}{\sum(\Delta)^2 - (1/)\sum^2 \Delta} \tag{23}$$

where ε is the residual of the model, Δ the overall variation of height of a given point (i.e. difference between the measured initial and final heights) and the number of points.

Note. Except when compaction is ignored, the correlation coefficient of the regression line of step 4 does not take into account the compaction step. Therefore it is not that of the overall model, given by Eq. (23).

4. Results and discussion

The first section of the results is the evaluation of the quality of the model, estimated by its correlation coefficient. After checking that the model simulates properly the variations of heights inside the plot, the second section studies some hydrological properties of the surfaces calculated with Eq. (13) and compares them to the observed ones.

The coefficients of compaction for the first rain after hoeing (Table 2) were calculated according to Eq. (16). In Fig. 4, the effect of compaction was ignored. The intercepts of the regression lines represent the mean variation in height and the slope represents the coefficient of Eq. (19). Table 3 repeats these results and, for the first rains after hoeing, shows the other results for each case (5 and 10 cm depth hoeing). The

Table 2
Mean variation of the plot heights during rainfall and resulting compaction coefficients for the two hypothesised depths of hoeing

	Rain 1				Rains 2 and 3	
	KD	MU	KU	MD	KD	MU
Δ (mm)	−16.6	−7.6	−13.6	−20.4	−0.2	0.3
γ (λ=10 cm) (%)	83	92	86	80	–	–
γ (λ=5 cm) (%)	67	85	73	59	–	–

coefficient of variation CV (the standard deviation over the mean), in the column at the right, expresses the dispersion of the adjusted values of and the mean correlation coefficient expresses the overall quality of the model in relation to the way compaction was treated. One can see that the hypothesis of soil work at 5 cm depth led to less dispersed coefficients and to higher coefficients of correlation than for the hypothesis of 10 cm depth. Both gave better results than when compaction was ignored. For the hypothesis of hoeing at 5 cm depth, the model explained between 61 and 82% of the variations of height during the first rain. The variance from 43 to 50% was explained by the model for the rains two and three.

The first achievement is the relatively good quality of the model used with regards to the simplicity of its governing processes and the basic simplicity of the numerical method used. A number of authors like Roth and Helming (1992) or Fox et al. (1998) have shown the complexity of existing interrelations between all the phenomena involved in microrelief evolution. In this context, we should notice the success, even relative, of a model based only on raindrop splash effect supposedly constant in time and space. This success can certainly be explained by the coarse texture of the studied soil and its poor cohesion. We also have to point out that was always calibrated. Trying to calculate from field data or equation adjustment of in time, instead of by calibration should be the next step of this work and could lead to lower coefficients of correlation.

Table 3
Adjusted values of the overall diffusion (Eq. (19)) and corresponding correlation coefficients of the model (Eq. (23)) when compaction is ignored or calculated on the hypothesis of a depth of hoeing of 5 and 10 cm

Compaction	KD	KU	MD	MU	
1					
					CV of (%)
Ignored	577	591	632	499	9.7
10 cm	508	540	545	465	7.1
5 cm	440	489	459	432	5.6
2					Mean of 2
Ignored (%)	54	65	68	58	62
10 cm	57	68	73	59	64
5 cm	63	74	82	61	70
2 3					
Ignored	373	–	–	471	
2					Mean of 2
Ignored (%)	43	–	–	50	46

The quality of the model is better for the first rain after hoeing because the soil surface has not already been reorganised at this stage and so, the situation is closer to the hypothesis of a uniform diffusion coefficient used in the model.

Besides raindrop erosion, on-site observation left no doubt as to the importance of a number of other processes which are listed below and in which the unexplained variance of the model can be looked at:

- . The available data allowed us to consider compaction only in a simplified way. The two major drawbacks were (a) the surface of the floor of the hoed layer was not a plane but followed the path of the teeth of the hoe and (b) the compaction was not uniform throughout the plot; the submerged areas were more compacted than the exposed ones.
- . The areas submerged under more than 1 cm depth were protected from raindrop impacts.
- . Small waves were generated by the impacts of raindrops. This agitation caused erosion at the edge of the puddles.

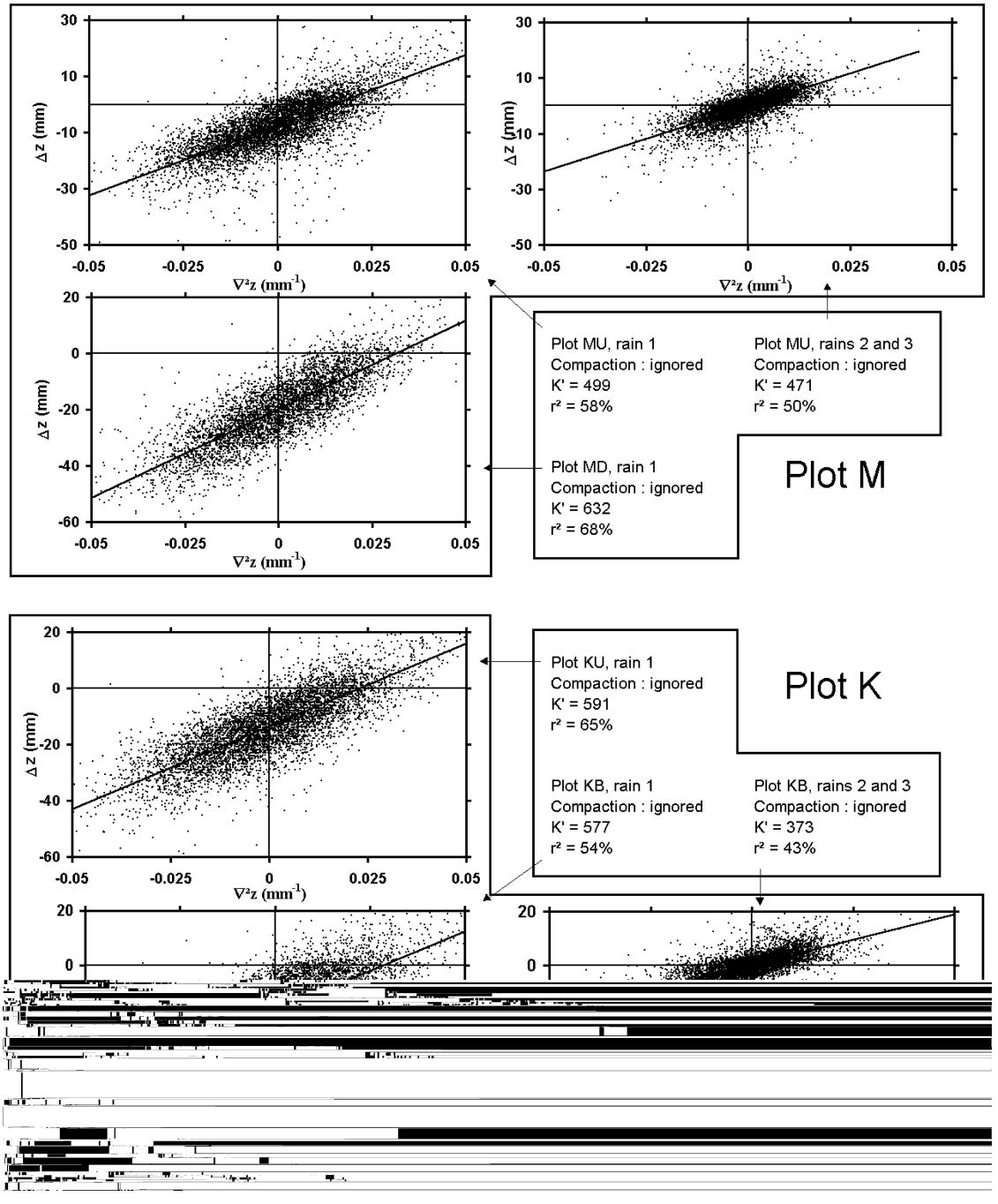

Fig. 4. Scatter-plots of Δ , the measured variations of heights, against ∇^2 , the Laplacian of heights before rainfall. , the overall diffusion (Eq. (19)), is the slope of the regression line of the scatter-plot.

- . The flow has its own erosive dynamics in shaping its channels.

For the rains two and three, was calculated on the total effect of the two rains and therefore, cannot be directly compared to the former values. Nevertheless, had it been possible to calculate it for each single rain, it would have been smaller. Therefore it seems clear that the diffusion coefficient decreased with the cumulated rainfall since hoeing. Such a decrease can certainly be attributed to the structural changes of the soil surface (Le Bissonnais, 1988; Valentin and Bresson, 1992). Elsewhere, the distance of projection of a given particle depends on its diameter (Savat and Posen, 1981) and this is another cause of surface reorganisation which interacts with raindrop erosion (Wainwright et al., 1995) and therefore increases the spatial variability of .

We have shown in the previous section that the diffusion equation can explain the evolution of microrelief during the rain. We have also shown that considering compaction, even roughly, improves noticeably the quality of the model. The overall evaluation of the model was made on the basis of its correlation coefficient. This section focuses on the hydrological properties of the simulated surfaces: RR, SSA and SSC. These properties were calculated on the modelled surfaces and compared to the corresponding observed surfaces. The results are shown in Table 4 and Fig. 5.

Table 4
Plot surface characteristics (RR: random roughness; SSA: specific surface area; SSC: surface storage capacity)

Plot	Surface	RR (mm)	SSA (%)	SSC (mm)
KD	After ploughing	17.0	11.2	9.7
	After rain 1	11.0	4.6	8.2
	After rain 3	9.5	3.1	6.2
MU	After ploughing	14.4	7.9	7.3
	After rain 1	10.4	3.4	5.1
	After rain 3	8.6	2.1	3.3
KU	Before ploughing	5.4	0.6	0.5
	After ploughing	14.9	10.9	12.5
	After rain 1	9.7	3.8	7.6
MD	Before ploughing	5.4	0.7	0.7
	After ploughing	13.1	9.7	12.0
	After rain 1	8.0	2.7	4.9

RR was underestimated by 0.8–2 mm; the simulated surfaces are smoother than real surfaces. This is a direct consequence of the partial explication of the variance of height variations by the model. SSA was equally underestimated. This parameter is linked to RR, the SSA of a smoother surface being logically lower.

SSC was overestimated. SSC is partially linked to RR (Huang and Bradford, 1990) and therefore was expected to be underestimated. But in fact the ridges,

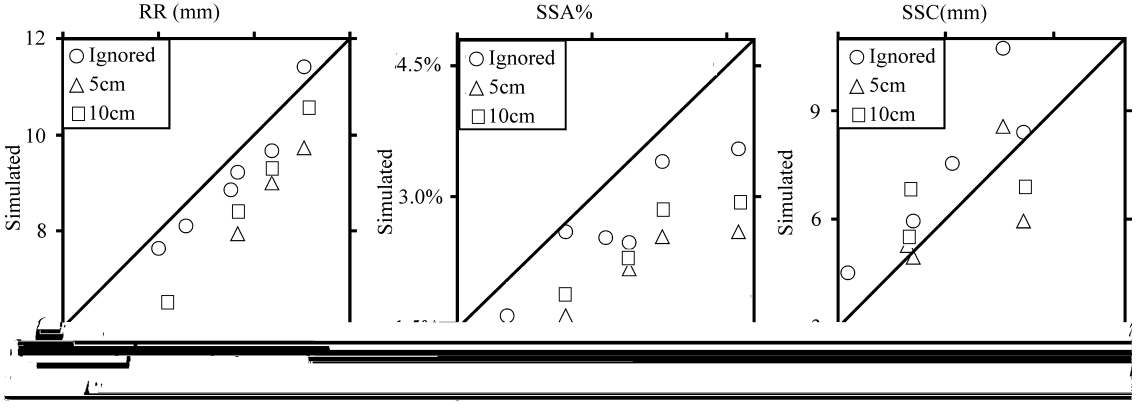

Fig. 5. Characteristics of simulated microrelief compared to observed ones when compaction is ignored or calculated on the hypothesis of a depth of hoeing of 5 and 10 cm.

which are perpendicular to the slope in this experiment, are crossed by the runoff. The role of runoff in the shaping on microrelief appeared to be decisive in the evolution of SSC despite the small size of the areas involved. This interaction between the soil and the water running on its surface is fundamental in the evolution of SSC. Since existing models are dedicated to the effect of runoff erosion at the square meter scale (Favis-Mortlock et al., 1998), coupling raindrop erosion and runoff erosion appear to be a promising approach towards an accurate simulation of the evolution of the shape of tillage-induced microreliefs during rainfall.

5. Conclusion

The research for a simple method to interpolate microrelief between two given dates led us to show that the effect of raindrop erosion on tillage-induced microreliefs can be represented by the diffusion equation. This issue was found to be both interesting and productive. It allowed us to demonstrate that raindrop erosion is in fact the dominant phenomenon in microrelief evolution during rainfall. Despite the complexity of the physical processes involved, a simple diffusion equation, with a calibrated coefficient of diffusion supposedly uniform and constant, led to an acceptable description of the resulting microreliefs.

Compaction occurred during the first rain after hoeing. The combination of compaction and raindrop erosion explained between 61 and 82% of the variance of heights variations on the plot. For the first rain after hoeing, the adjusted values of the total diffusion were close to each other despite differing initial conditions of moisture and microrelief. During the following rains, there was no more compaction but the soil surface was already reorganised by crusting. The diffusion equation with a uniform diffusion coefficient explained 43–50% of the variance. The diffusion coefficient appears to lessen with time, which agrees with previous works showing that the soil becomes more resistant to raindrop erosion as crusts develop.

There were two difficulties in using the diffusion equation in our initial objective of interpolating the surfaces between two rains. The first was the importance of compaction which dominates raindrop erosion during the first millimetres of rain. Compaction was difficult to take into account accurately because the depth of hoeing and the bulk density of the hoed layer were not precisely known. The second difficulty was that the runoff, despite the small quantities of soil displaced, had a decisive effect on the evolution of hydrological properties of soil surfaces, particularly on SSC.

In conclusion, it has been proved that the diffusion equation can be used to model the effect of raindrop erosion on tillage-induced microreliefs. This equation allows us to use a single diffusion coefficient to characterise the result of complex phenomena of detachment and transport by splashes. The first results, shown in this article, are promising and the diffusion equation will certainly find a useful application when coupled with other models simulating the effect of runoff if the derivation of the equation allows the diffusion coefficient to vary in time and if the experimental data allow us to estimate the diffusion coefficient and its variations in time.

Acknowledgements

The research for this paper was founded and carried out as a part of RIDES (Ruissellement Infiltration Détention et Etats de Surface) which is a core project of PNRH (the French National Program for Hydrological Research) and PHSE (the French National Program on Soil Erosion). The authors thank Dr. John Wainwright for his review of the paper and his helpful suggestions, Paul Mazoyer for his kind contribution to the improvement of the mechanics of the relief meter, and Kokou Abotsi for his decisive contribution to the conception and fabrication of the rainfall simulator.

References

Al Durrah, M.M., Bradford, J.M., 1982. The mechanism of raindrop splash on soil surfaces. Soil Sci. Soc. Am. J. 46 (5), 1086–1090.

Allmaras, R.R., Burwell, R.E., Larson, W.E., Holt, R.F., 1966. Total porosity and random roughness of the interrow zone as influenced by tillage. USDA Conservation Research Report No. 7, 22 pp.

Bjorneberg, D.L., Aase, J.K., Trout, T.J., 1997. WEPP model erosion evaluation under furrow irrigation. Annual International Meeting, Minneapolis, MI. American Society of Agricultural Engineering, Paper No. 97-2115.

Boardman, J., Favis-Mortlock, D. (Eds.), 1998. Modelling Soil Erosion by Water. Springer, NATO-ASI Series I-55, Berlin, 531 pp.

Boiffin, J., 1984. La dégradation structurale des couches superficielles du sol sous l'action des pluies. Ph.D. Thesis. Inst. Nat. d'Agronomie Paris-Grignon, Paris, France, 320 pp.

Currence, H.D., Lovely, W.G., 1970. The analysis of soil surface roughness. Trans. Am. Soc. Agric. Eng. 13, 710–714.

De Ploey, J., Savat, J., 1968. Contribution à l'étude de l'érosion par le splash. Zeitschrift für Geomorphologie 2, 174–193.

Esteves, M., Planchon, O., Lapetite, J.M., Silvera, N., Cadet P., 2000. The ''EMIRE'' large rainfall simulator: design and field testing. In: Parsons, A.J., Lascelles, B. (Eds.), Rainfall Simulation in Geomorphology. Earth Surf. Processes Landforms 25, 681–690.

Favis-Mortlock, D., Boardman, J., Parsons, T., Lascelles, B., 1998. Emergence and erosion: a model for rill initiation and development. In: Abrahart, R.J. (Ed.), Proceedings of the Third International Conference on GeoComputation (CD). University of Bristol, September 17–19, 1998.

Fox, D.M., Le Bissonnais, Y., Quetin, P., 1998. The implications of spatial variability in surface seal hydraulic resistance for infiltration in a mound and depression microtopography. Catena 32 (2), 101–114.

Helming, K., Römkens, M.J.M., Prasad, S.N., 1998. Surface roughness related processes of runoff and soil loss: a flume study. Soil Sci. Am. J. 62, 243–250.

Huang, C., Bradford, J.M., 1990. Depressional storage for Markov–Gaussian surfaces. Water Resour. Res. 26 (9), 2235–2242.

Jenson, S.K., Domingue, J.O., 1988. Extracting topographic structure from digital elevation data for geographic information system analysis. Photogram. Eng. Remote Sensing 54 (11), 1593–1600.

Jetten, V., de Roo, A., Favis-Mortlock, D., 1999. Evaluation of field-scale and catchment-scale soil erosion models. Catena 37 (3/4), 521–541.

Kamphorst, E.C., Jetten, V., Guérif, J., Pitkänen, J., Iversen, B.V., Douglas, J.T., Paz, A., 2000. Predicting depressional storage from soil surface roughness. Soil Sci. Soc. Am. J. 65.

Lacano, R.J., Vorheis, J.T., Baumhardt, R.L., Salisbury, D.R., 1997. Computer controlled variable intensity rain simulator. Soil Sci. Soc. Am. J. 61 (4), 1182–1189.

Le Bissonnais, Y., 1988. Analyse des mécanismes de désagrégation et de mobilisation des particules de terre sous l'action des pluies. Ph.D. Thesis. University of Orléans, 225 pp.

Le Bissonnais, Y., Benkhadra, H., Chaplot, V., Fox, D., King, D., Daroussin, J., 1998. Crusting, runoff and sheet erosion on silty loamy soils at various scales and upscaling from m^2 to small catchments. Soil Till. Res. 46, 69–80.

Magunda, M.K., Larson, W.E., Linden, D.R., Nater, E.A., 1997. Changes in microrelief and their effects on infiltration and erosion during simulated rainfall. Soil Technol. 10 (1), 57–67.

Moore, I.D., Larson, C.L., 1979. Estimating micro-relief surface storage from point data. Trans. Am. Soc. Agric. Eng. 22, 1073–1077.

Nearing, M.A., 1998. Why soil erosion models over-predict small soil losses and under-predict large soil losses. Catena 32, 15–22.

Perez, P., 1994. Genèse du ruissellement sur les sols cultivés du Sud du Saloum (Sénégal). Du diagnostic à l'aménagement de parcelle. Ph.D. Thesis. Ec. Nat. Sup. Agronomie Montpellier, ENSAM, Montpellier, 250 pp.

Planchon, O., Darboux, F., 2000. A fast, simple and versatile algorithm to fill in depressions in digital elevation models. In: Auzet, A.V., Poesen, J., Valentin, C. (Eds.), Soil Pattern as a Key Factor of Water and/or Wind Erosion. Catena, in press.

Planchon, O., Cadet, P., Lapetite, J.M., Silvera, N., Esteves, M., 2000a. Relationship between raindrop erosion and runoff erosion under simulated rainfall in the Sudano-Sahel. Consequences for the spread of nematodes by runoff. In: Parsons, A.J., Lascelles, B. (Eds.), Rainfall Simulation in Geomorphology. Earth Surf. Processes Landforms 25, 729–741.

Planchon, O., Esteves, M., Silvera, N., 2000b. Microrelief induced by tillage: measurement and modelling of surface storage capacity. In: Auzet, A.V., Poesen, J., Valentin, C. (Eds.), Soil Pattern as a Key Factor of Water and/or Wind Erosion. Catena, in press.

Roth, C.H., Helming, K., 1992. Dynamics of surface sealing, runoff formation and interrill soil loss as related to rainfall intensity, microrelief and slope. Z. Pflanzenernahr. Bodenk. 155 (3), 209–216.

Savat, J., Posen, J., 1981. Detachment and transportation of loose sediments by raindrop splash. Part I: The calculation of absolute data on detachability and transportability. Catena 8, 1–17.

Valentin, C., Bresson, L.M., 1992. Morphology, genesis and classification of soil crusts in loamy and sandy soils. Geoderma 55, 225–245.

Valentin, C., Bresson, L.M., 1997. Soil crusting. In: Lal, R., Blum, W.E.H., Valentin, C., Stewart, B.A. (Eds.), Methodology for Assessment of Soil Degradation. Advances in Soil Science. CRC Press, New York, pp. 89–108.

van Wesemael, B., Poesen, J., de Figueiredo, T., 1995. Effects of rock fragments on physical degradation of cultivated soils by rainflow. Soil. Till. Res. 33, 229–250.

Wainwright, J., Parsons, A.J., Abrahams, A.D., 1995. A simulation study of the role of raindrop erosion in the formation of desert pavements. Earth Surf. Processes Landforms 20, 277–291.

Zobeck, T.M., Onstad, C.A., 1987. Tillage and rainfall effects on random roughness: a review. Soil Till. Res. 9, 1–20.